Fissure Changes of Granite Video Image Using Fractional Differential

Jinming Xu, Xu Feng, Xiaohong Xu, and Binghua Chen

Abstract. The video images photographed in laboratory tests were used to investigate the fissure changes in granite. Frames were extracted out and investigated using the digital image processing. The intro-frame average technique was utilized to overcome the effects of sample trembles on the image processing. The locations of the micro compositions, especially those of new-generated fissures, were examined using fractional differential. The effects of the surrounding factors on the image properties were also examined. A criterion of image characteristic parameters for generating new fissures was furthermore proposed. The method proposed herein may be used as references in analyzing the physical mechanism of deformations and failures of rock materials or rock masses in rock regions.

1 Introduction

The conventional methods in investigating the fissures of a rock include the macro-scale measurements, finite element analyses, and laboratory tests. Nevertheless, a macroscopical measurement has the drawbacks such as the time consuming and low precision. The finite element method and laboratory test can not straightforwardly measure the locations of compositions.

Most approaches related to investigating the fissures in a rock may be divided into two categories: highlight either on the image information or on the geological features. As for the former category, Wang et al [2] presented the fractional differential masks and their numerical implementation algorithms; Yang [5] extracted the high-frequency signals by an iterative convoluted calculation; Xu et al [3] analyzed the textural parameters of limestone using video images. As for the latter

Jinming Xu · Xu Feng
Department of Civil Engineering, Shanghai University, Shanghai, China
e-mail: xjming@163.com

Xiaohong Xu · Binghua Chen
Shanghai Science and Technology Museum, Shanghai, China
e-mail: xuxiaohong85@163.com

Z. Qian et al. (Eds.): Recent Advances in CSIE 2011, LNEE 129, pp. 99–104.
springerlink.com

category, more attentions were paid to the geological features. For instance, Vajdov et al [1] investigated the modes and orientations of the microcrack initiation, propagation and coalescence, and failure modes of a limestone.

In the current study, by using the video images captured in the laboratory tests, the locations of fissures in rocks were determined using the fractal differential to examine the image features and their influencing factors in different load time and to propose a criterion for the initiation of fissures in rock materials.

2 Studied Regions in Video and Modifications of Trembles

The granite used in this study was collected in field. The sliced and polished treatments were conducted to produce the cubic specimens with a size of around 50×50×50 mm. In front of the specimen at a distance of about 50 cm, the tripods were fastened and amounted on three digital cameras with the HDR-XR150E type, produced by the SONY Company. The weight of each camera is 300 g with the size of 57×67×106 mm, lens of Vario Tessar, sensitization component of Exmor RCMOS. The effective pixels of the camera are 1350000 in dynamic mode using the electronic anti-shake system in enhanced mode. The lowest level of illuminance was 3 with the dynamic image of 1664×1244 pixels. The auto backlight compensation was utilized with the aperture size of F1.8 to F3.2. The uniaxial compression tests for the specimens were employed using the YE-2000 type of hydraulic machine, the test data was acquired using a Smart Test Computer-controlled System. A low loading speed was adopted until the rock failures.

All of the video images were taken from the normal surface of specimens with a MIS type and the screen transmission speed of 25 frames per second. Each frame of image was extracted from the video images. The accurate time of each frame was computed according the time interval of the video, load time and the time the test ends. For each frame, the original RGB type of frame was transformed into the corresponding gray and binary image, expressed as a discrete function $s_k(i, j)$, where R, G and B represent red, green, and blue, respectively; i and j are coordinates of each pixel; k=1, 2, 3 denote red, green and blue. The studied region was chosen as a little bigger than that of the fissures.

During capturing the video images, many influencing factors may cause sample trembles, including those induced from the camera itself, ground surface, and external load. The former two can be overcome either by changing the beginning time of tests or by improving the stability of the equipments, but there is no appropriate method at present for the third factor. In this study, the test time was chosen as one when there were almost no trembles around. The use of fastened tripods can avoid the trembles of cameras. The intro-frame average technique was utilized to overcome the effects of sample trembles.

In order to eliminate too bright or dark areas of a frame caused by surrounding luminance, the histogram equalization technique was conducted to each frame. The result images treated by the above methods were presented in Fig.1.

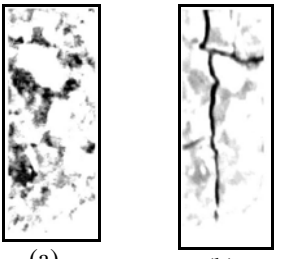
(a) (b)

Fig. 1 Result images of granite: (a) with no new-generated fissures; (b) with new-generated fissures

3 Use of Fractional Differential

The fissure regions can be extracted from the rock image [4] using the edge-detection techniques. To effectively analyze the propagation of new-generated fissures, a fractional differential was used to obtain the distributions of fissures.

Given $x \in [x_1, x_2]$ and $y \in [y_1, y_2]$ for a gray image $s(x,y)$, the approximate backward differentials of $s(x,y)$ in the x and y orientations may be expressed as

$$\frac{\partial^{\upsilon} s(x,y)}{\partial x^{\upsilon}} \approx s(x,y) + \sum_{n=1}^{n=+\infty} a_n s(x-n,y)$$

where

$$a_n = \frac{\Gamma(-\upsilon+1)}{n!\Gamma(-\upsilon+n+1)}, \quad a_0 = \frac{\Gamma(-\upsilon+1)}{0!\Gamma(-\upsilon+0+1)} = 1$$

where v is the order of the differential, and n is the size of masks. The masks of the fractional differential can be constructed according to the coefficients a_n shown in Fig. 2 (Pu and Wang, 2007).

a_n	0	0	...	0	a_n	0	...	0	0	a_n
0	a_{n-1}	0	...	0	a_{n-1}	0	...	0	a_{n-1}	0
...	...	...	...	...	...	...	...	...	...	...
0	...	0	a_2	0	a_2	0	a_2	0	...	0
0	...	0	0	a_1	a_1	a_1	0	0	...	0
a_n	a_{n-1}	...	a_2	a_1	a_0	a_1	a_2	...	a_{n-1}	a_n
0	...	0	0	a_1	a_1	a_1	0	0	...	0
0	...	0	a_2	0	a_2	0	a_2	0	...	0
...	...	...	...	...	...	...	...	...	...	...
0	a_{n-1}	0	...	0	a_{n-1}	0	...	0	a_{n-1}	0
a_n	0	0	...	0	a_n	0	...	0	0	a_n

Fig. 2 Masks of fractional differential

The order of fractional differential and the size of masks play an important role in the result image as the fractional differential was utilized to treat an image. The order and the masks of the fractional differential were chosen as 2.01 and a square with 5×5 pixels, respectively. The digital image $s(x,y)$ was convoluted using the masks, respectively, in the upward, downward, leftward, rightward, top-left di-

agonal, top-right diagonal, bottom-left and bottom-right directions. The result image of fractional differential were obtained by computing the average of the results in all of these eight directions and shown as Fig. 3(a).

4 Distributions and Propagations of Fissures

4.1 Determination of Fissure Locations

The conventional threshold technique was used herein in the extraction of the fissures. The threshold between fissures and other micro compositions was chosen as 65. The granite image after the fractional differential treatment presents in Fig.3(a). The result image after the threshold technique is shown as Fig.3(b).

It should be pointed out that the threshold of fissure distribution may be overlapped by that of other micro compositions. If the threshold technique was only used, some parts of the fissures may be wrongly recognized as other micro compositions, and vice versa. If some of the morphological methods were used, the narrow gap between micro compositions may be eliminated. Nevertheless, the size of fissure regions may be changed if the morphological analyses were used, resulting to the total percentage of micro compositions of less than 100. Therefore, the morphological analyses were not utilized in the current study.

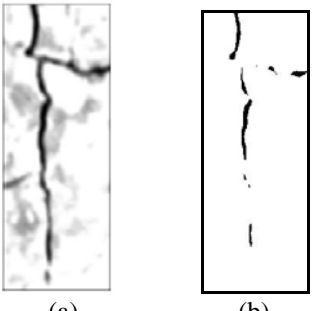

Fig. 3 Newly-generated fissure distributions in granite image: (a) using fractional differential treatment; and (b) using threshold technique

4.2 Extraction of Fissure Parameters

After fissure distributions were determined, the parameters of each fissure were computed, including the eccentricity, perimeter, number of regions, size of the area, coordinates of the centroid, equivalent diameter of a circle, value and direction of long-axis and short-axis, and so on. The relations among these parameters, initiations and changes of newly-generated fissures may be established. The corresponding digital criterion for generating new fissures may be thereafter obtained. It was found that the eccentricity and long-axis direction of the fissure distributions reflected the fissure features and their changes with the external loads.

4.3 Change in Fissure Parameters

The initiation and propagation of fissures and the failure of the rock generally occurred near the end of the video image. The initiation criterion of fissures in the rock was obtained by investigating the changes of configuration parameters of fissure distributions with time or with load. Figs. 4 and 5 are the change curve of the eccentricities and the directions of long-axis of the fissures, respectively.

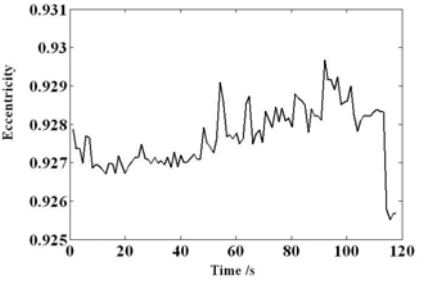

Fig. 4 Eccentricities of fissures in different time

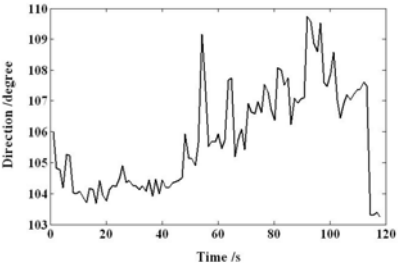

Fig. 5 Directions of long-axis of fissures in different time

From Fig.4, it can be seen that the eccentricity of fissures in granite image rapidly reduced to a low level at the 116th second, and, as a result, many fissures should occur at this time; whereas eccentricity of fissures was still at a low level and the rock failure at the 118th second. From Fig.5, the directions of fissures changed gradually until the rock failures. However, an obvious mutation occurred between the 116th and 118th seconds during the test. This agrees with that observed in the video image.

5 Summary

1. The locations of fissures in granite were obtained using the fractional differential in the current study. The vision of the fissure in the image was improved if the masks of fractional differential were utilized. During generating new fissures, the characteristic parameters of the image had an obvious change.
2. The initiation criterion of newly-generated fissures was established using the eccentricities of fissures and the directions of long-axis of fissures in different time. The main influencing factors of characteristic parameters were furthermore investigated for the granite image.

3. The establishments of a digital characteristic parameter system for the rock fissures and of the recognizing criterion of generating new fissures need to be further investigated.

Acknowledgements. Financial supports for the study were provided by the Natural Sciences Foundation Committee of China under Grant No.405712191 and by the Shanghai Municipal Education Commission under Grant No.09YZ39. These supports were gratefully acknowledged. The authors are grateful to the anonymous reviewers for their valuable suggestions in the preparation of this paper.

References

1. Vajdov, V., Zhu, W., Chen, T.M.N., Wong, T.F.: Micromechanics of brittle faulting and cataclastic flow in Tavel limestone. J. Struct. Geol. 32, 1158–1169 (2010)
2. Wang, W.X., Yu, X., Lai, J.: Image enhancement for rock fractures based on fractional diferential. J. Comput. Appl. 29, 3015–3017 (2009) (in Chinese)
3. Xu, J., Han, N.N., Li, Y.: Digital features of localized deformation of limestone. Chin. J. Rock Mech. & Eng. 29, 2110–2115 (2010) (in Chinese)
4. Xu, J., Zhao, X., Liu, B.: Digital image analysis of fluid inclusions. Int. J. Rock Mech. & Min. Sci. 44, 942–947 (2007)
5. Yang, Z.: An amage extraction algorithm for rock fractures on fractional differential. Comput. & Inf. Tech. 17, 6–8 (2009) (in Chinese)